ADVANCED FUNCTIONAL MATERIALS
www.afm-journal.de

Magnetic Helical Microswimmers Functionalized with Lipoplexes for Targeted Gene Delivery

Famin Qiu, Satoshi Fujita, Rami Mhanna, Li Zhang, Benjamin R. Simona, and Bradley J. Nelson**

Artificial micro-/nanoswimmers have various potential applications including minimally invasive diagnosis and targeted therapies, environmental sensing and monitoring, cell manipulation and analysis, and lab-on-a-chip devices. Inspired by natural motile bacteria such as *E. Coli*, artificial bacterial flagella (ABFs) are one kind of magnetic helical microswimmers. ABFs can perform 3D navigation in a controllable fashion with micrometer precision under low-strength rotating magnetic fields (<10 mT) and are promising tools for targeted drug delivery in vitro and in vivo. In this work, the successful wirelessly targeted and single-cell gene delivery to human embryonic kidney (HEK 293) cells using ABFs loaded with plasmid DNA (pDNA) in vitro is demonstrated for the first time. The ABFs are functionalized with lipoplexes containing pDNA to generate functionalized ABFs (f-ABFs). The f-ABFs are steered wirelessly by low-strength rotating magnetic fields and deliver the loaded pDNA into targeted cells. The cells targeted by f-ABFs are successfully transfected by the transported pDNA and expressed the encoding protein. These f-ABFs may also be useful for in vivo gene delivery and other applications such as sensors, actuators, cell biology, and lab-on-a-chip environments.

1. Introduction

Artificial micro-/nanoswimmers are currently an active research field due to their various potential applications, ranging from modern biomedical applications such as minimally invasive surgery and targeted therapy,[1–7] manipulation of micro-/nano-objects,[8,9] to environmental applications such as decontamination and toxicity screening.[10–12] Micro-/nanoswimmers with different propulsion mechanisms have been developed.[13] The use of magnetic fields to power micro-/nanoswimmers has gained particular interest, especially in biomedical applications, since the magnetic fields can penetrate through the human body allowing wireless control of these tiny devices without harming cells and tissues.[6,14]

In nature, bacteria such as *E. coli* swim in viscous fluids by rotating flagella in a helical wave to propel themselves.[15] Inspired by this flagellar propulsion method, magnetic micro-/nanoswimmers with helical shapes have been fabricated by different methods such as glancing angle deposition (GLAD),[16] self-rolling techniques,[17,18] 3D lithography,[19] and biotemplate methods.[20] Artificial bacterial flagella (ABFs)[21] are one type of magnetic helical microswimmers with helical shapes and magnetic materials. ABFs can perform 3D navigation in a controllable fashion with micrometer precision in liquid using low-strength rotating magnetic fields translating rotational movement to translational motion in a screw-like fashion. This flagellar propulsive method has been proposed as a promising approach for in vivo applications.[2,22]

Previous work showed that ABFs can manipulate and transport microbeads in 3D.[19] For biomedical applications, ABFs were shown to be noncytotoxic after 72 h of incubation with mouse muscle cells,[23] and the functionalization of ABFs with nanosized drug carriers, i.e., liposomes, has been studied. The abilities of controlled release and single-cell targeted delivery with these liposome-functionalized ABFs (f-ABFs) have been demonstrated by capturing a water-soluble drug model molecular (calcein) within liposomes.[24,25]

Gene therapy is a medical treatment in which DNA is used as a therapeutic drug that is delivered into a patient's cells to treat diseases such as inherited disorders and cancers. During

F. Qiu, Prof. B. J. Nelson
Institute of Robotics and Intelligent System (IRIS)
ETH Zurich, Zurich CH-8092, Switzerland
E-mail: bnelson@ethz.ch
Dr. S. Fujita
Biomedical Research Institute
AIST, 1-1-1 Higashi, Tsukuba, Ibaraki 305-8566, Japan
Dr. S. Fujita, B. R. Simona
Laboratory of Biosensors and Bioelectronics
University and ETH Zurich
Zurich CH-8092, Switzerland
Dr. R. Mhanna
Biomedical Engineering
American University of Beirut
Beirut 1107 2020, Lebanon
Prof. L. Zhang
Department of Mechanical and Automation Engineering
The Chinese University of Hong Kong
Hong Kong SAR, China
Prof. L. Zhang
Chow Yuk Ho Technology Centre for Innovative Medicine
The Chinese University of Hong Kong
Hong Kong SAR, China

DOI: 10.1002/adfm.201403891

the process the nucleic acids must be delivered to the defect cells, transfected into the cells, and then express a function to treat a particular disease. Gene delivery carriers, commonly called vectors, have been developed to carry the DNA to improve gene therapy due to the poor efficiency of naked DNA entering cells. Lipoplexes, complexes of cationic lipids and DNA, are one promising tool for nucleic acid delivery to cells, such as for delivering siRNA for gene silencing and plasmid DNA (pDNA) for transfection.[26–29] The delivery of nucleic acids to targeted cells and tissues remains a challenge.[26] By integrating lipoplexes with mobile microrobots such as ABFs as lipoplex carriers, a multifunctional system can be created that can be wirelessly controlled for targeted delivery of DNA to specific areas in hard-to-reach areas, such as in the human body or in lab-on-a-chip environments.

In this work, we demonstrated for the first time successful wirelessly targeted and single-cell gene delivery to human embryonic kidney (HEK 293) cells using ABFs loaded with a lipoplex in vitro. As a result of development of our reverse transfection technology,[30] the lipoplex was successfully bound to ABFs and was only released into cells by contact between ABFs and cells. pDNA was first mixed and complexed with lipofectamine 2000, a cationic lipid, to form the lipoplex. The functionalization of ABFs with the lipoplex was characterized by the fluorescent probe method. The f-ABFs were steered and controlled wirelessly by low-strength rotating magnetic fields and the loaded pDNA was delivered into targeted cells. The lipoplex containing pDNA carried by f-ABFs was taken up only by the targeted cells. Successful gene transfection and gene expression to encoding proteins by the targeted cells were verified.

2. Results and Discussion

2.1. Fabrication of ABFs

The ABFs were fabricated using 3D laser direct writing tool and e-beam deposition methods.[19] Using these methods, a large number of ABFs (10 000 ABFs) can be produced in batch. A single ABF is 5 μm in diameter and 16 μm in length (**Figure 1**). Each ABF has a polymeric body inside and a metallic Ni/Ti (25 nm/15 nm) bilayer on the surface. The magnetic Ni layer enables us to wirelessly control the swimmers navigation in 3D in liquid using low-strength rotating magnetic fields (<10 mT),

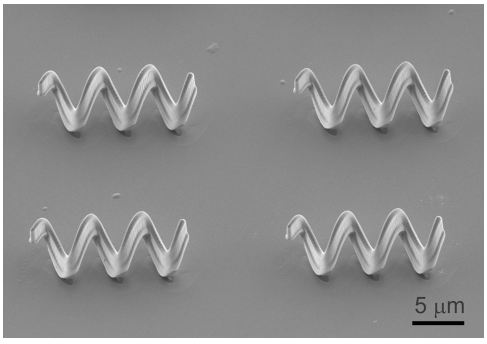

Figure 1. SEM image of four ABFs on a glass substrate imaged by a SE2 detector.

and the Ti layer has three main advantages: (1) preventing the Ni from oxidation,[23] (2) improving the biocompatibility of the structures,[19,31,32] and (3) facilitating the surface functionalization of the structures with other medical and biological substances such as liposomes.[24,25]

2.2. Functionalization of ABFs with Lipoplexes

Lipofectamine 2000 was used as the cationic lipids to mix with pDNA. Lipofectamine 2000 is a commercially available cationic reagent that provides highly efficient transfection of nucleic acids (DNAs or RNAs) into a wide range of mammalian cells.[33] While the detailed chemical composition of the reagent is not disclosed by the provider, the mixing of the cationic lipids of lipofectamine 2000 and the anionic nucleic acids generates cationic lipoplexes through ionic interactions. The lipoplexes easily fuse with the negatively charged cell membrane or are incorporated into cells by endocytosis, which facilitate the transport of DNA through the cell membrane and also protect the DNA from undesirable degradation.[34,35]

Cell adhesive proteins, fibronectin and gelatin, were added into the mixture of lipofectamine 2000 and pDNA to form the final lipoplex, since previous results showed that these proteins are important for local and highly efficient transfection of lipoplexes in the reverse transfection technology.[30] Fibronectin, is an extracellular matrix component that binds to integrins on cell membranes, provides a scaffold for cells and ensures strong cellular adhesion on solid surfaces such as glass, metal, etc.[30,36] Strong cellular adhesion on solid surfaces promotes gene transfection by contact between lipoplexes and cellular membrane. Moreover, gelatin adsorbs aqueous mixtures including lipoplexes and suppresses their release from solid surfaces.[37] The detailed component of the lipoplex is shown in **Table 1**, and the detailed preparation process can be found in the Experimental Section.

The outer Ti surface of ABFs was oxidized to be TiO_2, therefore, a TiO_2-coated crystal was used as a model to test the absorption of the lipoplex by quartz crystal microbalance with dissipation monitoring (QCM-D). QCM-D is a commonly used tool to measure adsorption of lipids and their structure on surfaces.[38] Lipids adsorbed on the surface of a QCM-D crystal cause a drop in the measured resonant frequency and an increase in the dissipation of the crystal. By monitoring frequency and dissipation changes, the adsorption condition of the lipids on the surface can be tested. The QCM-D results show that the frequency shift dropped and the dissipation shift increased dramatically once the lipoplex was injected into the

Table 1. The components of the final lipoplex (50 μL in total).

Materials	Amount [μL]
Lipofectamine 2000	4
pDNA (pVenus-N1) (1 μg μL^{-1} in DW)	2
DMEM without phenol red	31.5
Gelatin (20 μg μL^{-1} in DW)	2.5
Fibronectin (4 μg μL^{-1} in PBS)	10

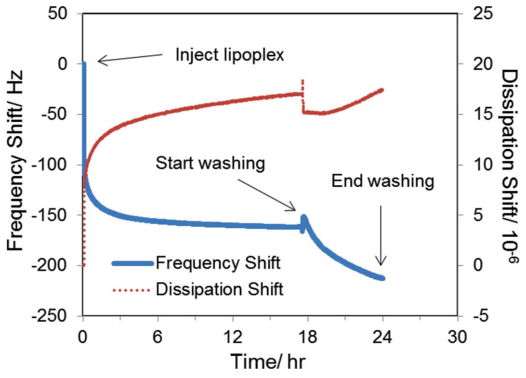

Figure 2. QCM-D measurement of the frequency and dissipation response to the adsorption of the lipoplex on a TiO_2 crystal. The HEPES sodium buffer was used for washing. Only the third overtones are shown for the sake of clarity.

chamber, which indicated good adsorption of the lipoplex onto the TiO_2 surface (**Figure 2**). The adsorption reached the maximum after incubation for 3 h. When HEPES sodium buffer was loaded onto the substrate for washing after lipoplex was absorbed on substrate for 18 h, the frequency shift decreased and the dissipation shift increased. The decrease of the frequency may come from the continuous adsorption of the substances remaining in the pump tube which were pumped into the chamber when starting the washing.

The functionalization of ABFs was performed by mixing the suspension of ABFs with the lipoplex. The mixture was incubated at room temperature for 3 h (from the QCM-D data) followed by washing to generate f-ABFs (**Figure 3**a). In order to confirm the successful loading of pDNA on the real ABF surface, we used pDNA labeled with fluorescein, a green fluorescent (Label IT Plasmid Delivery Control, Fluorescein; Mirus Bio LLC, Madison, WI) as a fluorescent probe. The fluorescent signals were verified by confocal laser scanning microscope (CLSM) after coating the lipoplex on ABFs. The green fluorescent signal detected around the ABF indicates the lipoplex loaded with pDNA was successfully coated and loaded on the ABF surface by the electrostatic force between the negatively charged TiO_2 surface of ABFs and the positively charged lipoplex (Figure 3).[35]

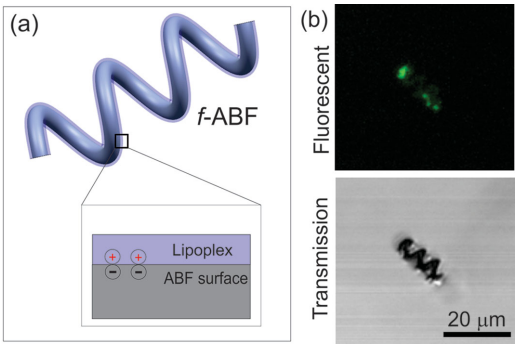

Figure 3. Functionalization of ABFs with the lipoplex. a) The schematic of the functionalization of ABFs with the lipoplex. b) The fluorescent and transmission images of a f-ABF by CLSM. The pDNA was marked using green fluorescence (fluorescein).

2.3. Swimming Performance of f-ABFs

Figure 4a shows the wirelessly controlled swimming performance of f-ABFs in cell medium under 5 mT rotating magnetic fields. The forward swimming speed of f-ABFs increased almost linearly as the rotating frequency of the magnetic fields increased and then reached the peak at the step-out frequency, i.e., the maximum frequency that swimmers can synchronize with the input frequency.[17,21,39] When the input frequency became higher than the step-out frequency of the swimmers, the swimming speed of the f-ABFs decreased dramatically. The average maximum forward speed of three tested f-ABFs (F-ABF1, F-ABF2, and F-ABF3) was 43.9 ± 1.3 μm s^{-1}, and the average step-out frequency was 31 ± 3 Hz. Figure 4b shows the wireless targeting ability of an f-ABF in vitro. The f-ABF was controlled to swim toward the target cell (cell 3) and contacted the cell (the inset of Figure 4b) by wireless means (see Video S1, Supporting Information).

2.4. Gene Transfection and Protein Expression

The transfection efficiency of the lipoplex was investigated using HEK 293 cells. Two different quantities of lipoplexes with pDNA encoding yellow–green fluorescent Venus protein [0.2 μg of pDNA (**Figure 5**a) and 1 μg of pDNA (Figure 5b)] were prepared. Then each lipoplex was added to 500 μL of DMEM with HEK 293 cells in a 24-well culture plate for gene transfection. The results show that 1 μg of pDNA as a component of the lipoplex is sufficient to transfect most of cells in 500 μL of cell medium in 23 h (Figure 5b).

Gene transfection of f-ABFs was then conducted. The f-ABF suspension was added to 500 μL of DMEM with the HEK 293 cells in one well of a glass-bottom 24-well plate. The f-ABFs deposited on HEK 293 cells on the bottom of the plate. After 16 h of incubation, the two cells contacting and/or neighboring one f-ABF became transfected with pDNA and presented a strong fluorescent signal from Venus proteins (**Figure 6**, Figure S1 and Videos 2 and 3, Supporting Information). The two transfected cells were daughter cells from a parent cell that had contacted and been transfected with pDNA from the f-ABF. This is indicated by the morphologies of the two cells expressing Venus protein that migrated separately after the division (Figure 6e). Successful protein expression indicates that the pDNA carried by ABFs was transferred into the membrane of the parent cells and imported into the nuclei through the temporarily compromised nuclear membrane during cell division. Venus proteins were then expressed in the daughter cells.

The absence of fluorescent signal from cells surrounding the daughter cells shows that the transfection from f-ABFs was locally limited to the contacted cells (Figure 6a–d). Figure S1, Supporting Information, shows two daughter cells that migrated and were separated by a greater distance after 48 h of incubation (Figure S1d–f) than after 16 h (Figure 6 and Figure S1a–c, Supporting Information), which indicates that the f-ABF was able to transfect the contact cells and did not influence cell division and migration. The cells underneath or surrounding of f-ABFs appear healthy in the transmission images (Figure S1a,d, Supporting Information), and the f-ABFs appear

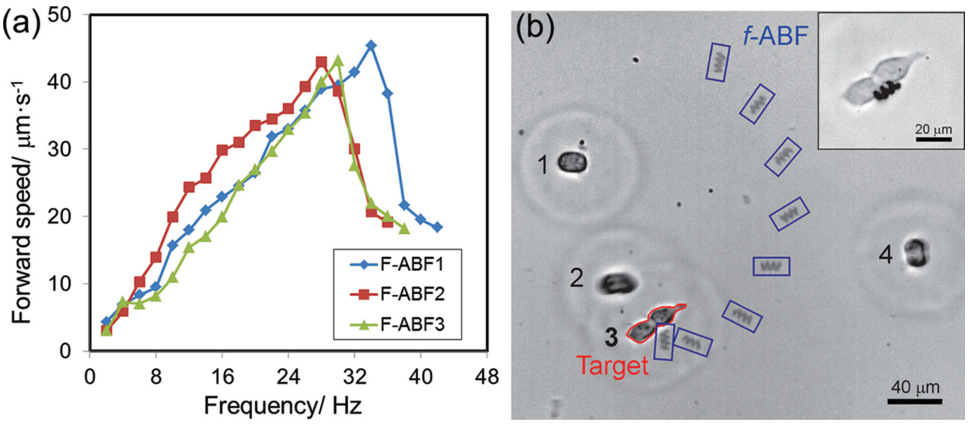

Figure 4. The wirelessly controlled swimming performance of f-ABFs in cell medium. a) The forward swimming speeds of three tested f-ABFs (F-ABF1, F-ABF2, and F-ABF3) as a function of input rotating frequency under 5 mT magnetic fields. b) Time-lapse photo of the controlled actuation of a f-ABF to the target cell (cell 3, the contour is circled in red). Cell 3 was under cell division and was considered as one single cell in this case. Cell 2 and cell 4 are blurred in the image due to the drift of cells in the medium during the time-lapse image. The movement of the f-ABF was marked with blue rectangles. The interval of each movement was 4 s. The inset shows a f-ABF in contact with cell 3.

to be nontoxic to human embryonic kidney (HEK 293) cells after two days.

3. Conclusion

Magnetic helical microswimmers were surface-functionalized with lipoplexes loaded with pDNA to generate f-ABFs. The f-ABFs can be precisely actuated by low-strength rotating magnetic fields, which are safe and nonharmful to cells and tissue, and controllably move to specific HEK 293 cells in vitro. The cells contacting f-ABFs were successfully transfected by the transported pDNA and expressed the encoding Venus protein. Beyond in vitro gene delivery applications, the possibility of f-ABFs targeting hard-to-reach areas in the human body can be envisaged, since the flagella-propulsive method is a promising approach for in vivo applications. These f-ABFs may also be useful in other applications, such as sensors, actuators, cell biology, and lab-on-a-chip environments.

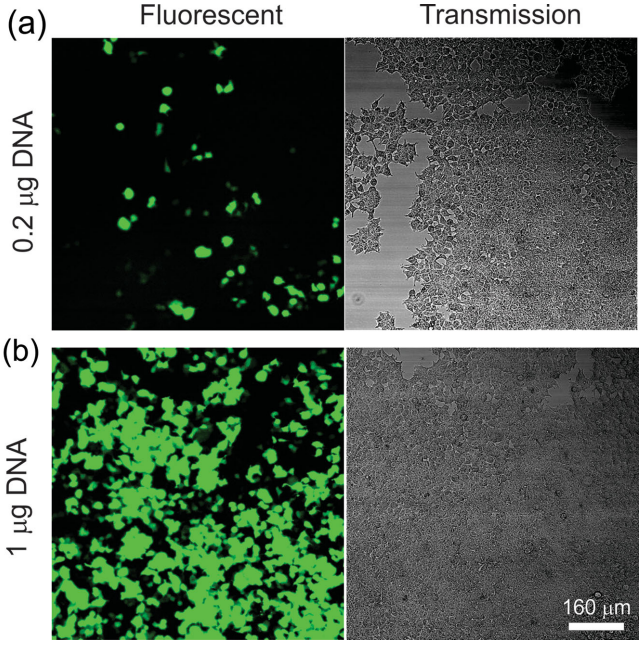

Figure 5. The transfection efficiency tests of the lipoplex after incubation of 23 h with two different pDNA amounts. a) 0.2 μg pDNA was added into the cell medium. b) 1 μg pDNA was added into the cell medium.

4. Experimental Section

Materials: Lipofectamine 2000 (Life technologies, Carlsbad, CA), bovine fibronectin (Life Laboratory Company, Yamagata, Japan), gelatin (Sigma-Aldrich, St. Louis, Madison, MO), Label IT Plasmid Delivery Control (Fluorescein; Mirus Bio LLC, WI), HEK 293 cells (American Type Culture Collection, Manassas, VA), fetal bovine serum (FBS; Life technologies), Dulbecco's modified eagle's medium (DMEM; Life Technologies), DMEM without phenol red (Life Technologies), antibiotic-antimycotic (100×; Life Technologies), HEPES sodium buffer (10×10^{-3} M 4-(2-hydroxyethyl)piperazine-1-ethane-sulfonic acid

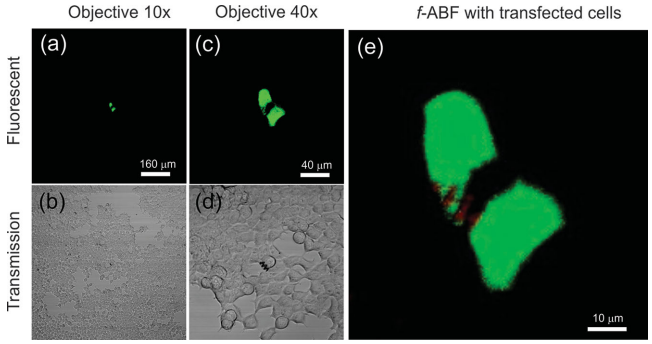

Figure 6. pDNA transfection and protein expression by the cells that contacted f-ABFs. a,b) and c,d) show the fluorescent and transmission images of cells with the f-ABF at 10× and 40× magnifications, respectively. e) The zoomed overlay of fluorescent and transmission images. The f-ABF (the red helix) is false-colored in red, processed using ImageJ software.

and 150 × 10^{-3} M NaCl in distilled water; MicroSelect, Fluka Chemie GmbH, Switzerland), DPBS (Dulbecco's phosphate-buffered saline; Life Technologies), trypsin–EDTA (0.05%; Life Technologies), and sodium chloride (NaCl; Sigma-Aldrich) were purchased. The pDNA encoding Venus protein was a gift from Advanced Industrial Science and Technology, Ibaraki, Japan.

Fabrication of ABFs: The helical bodies were fabricated in IP-L photoresist using a direct laser writing tool (Nanoscribe, from Nanoscribe GmbH) on a transparent glass substrate, and followed by coating with 25 nm Ni and 15 nm Ti using an electron beam evaporator (Plassys-II MEB550SL). The detailed fabrication information can be found in our previous literature.[19,24]

Preparation of the Final Lipoplex: First, a solution of pDNA (2 μL, 1 μg μL^{-1} fluorescein labeled one or Venus encoding one in distilled water (DW)), lipofectamine 2000 (4 μL), and DMEM (31.5 μL) were mixed and incubated for 20 min at room temperature. Gelatin (2.5 μL, 20 μg μL^{-1} in DW) and fibronectin (10 μL, 4 μg μL^{-1} in PBS) were added in the mixture. The components of the final lipoplex are shown in Table 1.

QCM-D Experiments: The TiO_2-coated crystal (Q-Sense, Sweden) was treated with UV/ozone cleaner for 30 min and loaded into the QCM-D chamber (Q-Sense E4, Gothenburg, Sweden). HEPES sodium buffer was injected into the chamber until a stable baseline was observed.[24] After that, the lipoplex (500 μL) (prepared as indicated in Table 1), was loaded in the chamber with a flow rate of 0.2 mL min^{-1}. After 13 h of incubation, the substrate was washed by HEPES sodium buffer with the speed of 0.1 mL min^{-1}.

Functionalization of ABFs with Lipoplexes: The fabricated ABFs were cleaned using UV/ozone cleaner for 30 min and released from the glass substrate in HEPES sodium buffer by sonication for 4 min at 56 kHz.[24] The ABF suspension was condensed to 50 μL by centrifuging. The lipoplex solution (50 μL) and the ABF suspension were mixed and incubated at room temperature for 3 h. In order to remove the uncoated lipoplex in the solution, we washed the mixture three times in HEPES sodium buffer (1 mL) and one time in DMEM (1 mL) by centrifuging the solution (4000 rpm, 3 min each time). The final f-ABF suspension in DMEM was condensed to 100 μL by centrifuging for further experiments.

Cell Culture: The DMEM supplemented with 10% fetal bovine serum and 1× antibiotic–antimycotic was used as the cell medium. We suspended 2 × 10^5 cells of HEK 293 in 500 μL of medium for seeding in one well of a 24-well culture dish with a glass bottom for the gene expression experiments and on a glass substrate for the swimming experiments.

Swimming Experiments: The swimming tests were conducted using rotating magnetic fields. The rotating magnetic fields are generated by a three-orthogonal-pair Helmholtz coil setup. The glass substrate with HEK 293 cells was placed in a tank (3 cm height, 1.5 cm width, and 3 mm height), which was filled with cell medium. The tank was placed in the center of the coil setup. A microscope with a camera was mounted above the tank. More details about the coils setup can be found in previous publications.[17,40] The swimming experiments with cells were completed within 1 h after the cells were taken from an incubator. After f-ABFs targeted and contacted cells, the cells were immediately put back into the incubator.

Gene Expression: The f-ABF suspension (50 μL) was added into HEK 293 cell medium (500 μL of DMEM supplemented with 10% fetal bovine serum and 1× antibiotic–antimycotic). The cells were incubated in CO_2 incubator at 37 °C for 16–48 h for gene transfection and protein expression. The fluorescent images were acquired using a CLSM (Carl Zeiss AG/LSM 510 with 10×, 20×, 40× 0.6 NA objectives and a 488 nm argon laser).

Supporting Information

Supporting Information is available from the Wiley Online Library or from the author.

Acknowledgements

The authors thank Prof. Janos Vörös (Laboratory of Biosensors and Bioelectronics, University and ETH Zurich, Switzerland) for his discussions. The authors also thank Yun Ding (Institute of Chemical and Bioengineering, ETH Zurich) for his discussions about the coating procedure, and the FIRST lab of ETH Zurich for technical support. Funding for this research was partially provided by the European Research Council Advanced Grant "Microrobotics and Nanomedicine (BOTMED)," the Swiss National Science Foundation (SNSF) Project No. 200021-130069, and the National Natural Science Funds of China (NSFC) for Young Scholar with Project No. 61305124.

Received: November 4, 2014
Revised: December 22, 2014
Published online: January 22, 2015

[1] B. J. Nelson, I. K. Kaliakatsos, J. J. Abbott, *Annu. Rev. Biomed. Eng.* **2010**, *12*, 55.
[2] K. E. Peyer, S. Tottori, F. Qiu, L. Zhang, B. J. Nelson, *Chem. Eur. J.* **2013**, *19*, 28.
[3] J. Wang, W. Gao, *ACS Nano* **2012**, *6*, 5745.
[4] L. Zhang, T. Petit, K. E. Peyer, B. J. Nelson, *Nanomed.: NBM* **2012**, *8*, 1074.
[5] S. Balasubramanian, D. Kagan, C.-M. Jack Hu, S. Campuzano, M. J. Lobo-Castañon, N. Lim, D. Y. Kang, M. Zimmerman, L. Zhang, J. Wang, *Angew. Chem.* **2011**, *123*, 4247.
[6] S. Fusco, M. S. Sakar, S. Kennedy, C. Peters, R. Bottani, F. Starsich, A. Mao, G. A. Sotiriou, S. Pané, S. E. Pratsinis, D. Mooney, B. J. Nelson, *Adv. Mater.* **2014**, *26*, 952.
[7] V. Garcia-Gradilla, J. Orozco, S. Sattayasamitsathit, F. Soto, F. Kuralay, A. Pourazary, A. Katzenberg, W. Gao, Y. F. Shen, J. Wang, *ACS Nano* **2013**, *7*, 9232.
[8] G. Zhao, H. Wang, S. Sanchez, O. G. Schmidt, M. Pumera, *Chem. Commun.* **2013**, *49*, 5147.
[9] T.-Y. Huang, F. Qiu, H.-W. Tung, X.-B. Chen, B. J. Nelson, M. S. Sakar, *Appl. Phys. Lett.* **2014**, *105*, 114102.
[10] W. Gao, J. Wang, *ACS Nano* **2014**, *8*, 3170.
[11] J. Orozco, G. Cheng, D. Vilela, S. Sattayasamitsathit, R. Vazquez-Duhalt, G. Valdés-Ramírez, O. S. Pak, A. Escarpa, C. Kan, J. Wang, *Angew. Chem. Int. Ed.* **2013**, *52*, 13276.
[12] J. Orozco, V. García-Gradilla, M. D'Agostino, W. Gao, A. Cortés, J. Wang, *ACS Nano* **2012**, *7*, 818.
[13] P. L. Venugopalan, R. Sai, Y. Chandorkar, B. Basu, S. Shivashankar, A. Ghosh, *Nano Lett.* **2014**, *14*, 1968.
[14] R. S. M. Rikken, R. J. M. Nolte, J. C. Maan, J. C. M. van Hest, D. A. Wilson, P. C. M. Christianen, *Soft Matter* **2014**, *10*, 1295.
[15] H. C. Berg, R. A. Anderson, *Nature* **1973**, *245*, 380.
[16] A. Ghosh, P. Fischer, *Nano Lett.* **2009**, *9*, 2243.
[17] L. Zhang, J. J. Abbott, L. X. Dong, B. E. Kratochvil, D. Bell, B. J. Nelson, *Appl. Phys. Lett.* **2009**, *94*, 064107.
[18] S. Schuerle, S. Pané, E. Pellicer, J. Sort, M. D. Baró, B. J. Nelson, *Small* **2012**, *8*, 1498.
[19] S. Tottori, L. Zhang, F. Qiu, K. K. Krawczyk, A. Franco-Obregón, B. J. Nelson, *Adv. Mater.* **2012**, *24*, 811.
[20] W. Gao, X. Feng, A. Pei, C. R. Kane, R. Tam, C. Hennessy, J. Wang, *Nano Lett.* **2013**, *14*, 305.
[21] L. Zhang, J. J. Abbott, L. Dong, K. E. Peyer, B. E. Kratochvil, H. Zhang, C. Bergeles, B. J. Nelson, *Nano Lett.* **2009**, *9*, 3663.
[22] J. J. Abbott, K. E. Peyer, M. C. Lagomarsino, L. Zhang, L. X. Dong, I. K. Kaliakatsos, B. J. Nelson, *Int. J. Robotics Res.* **2009**, *28*, 1434.
[23] F. Qiu, L. Zhang, K. E. Peyer, M. Casarosa, A. Franco-Obregon, H. Choi, B. J. Nelson, *J. Mater. Chem. B* **2014**, *2*, 357.

[24] F. Qiu, R. Mhanna, L. Zhang, Y. Ding, S. Fujita, B. J. Nelson, *Sens. Actuators B* **2014**, *196*, 676.
[25] R. Mhanna, F. Qiu, L. Zhang, Y. Ding, K. Sugihara, M. Zenobi-Wong, B. J. Nelson, *Small* **2014**, *10*, 1953.
[26] C. Tros de Ilarduya, Y. Sun, N. Düzgüne , *Eur. J. Pharm. Sci.* **2010**, *40*, 159.
[27] Z. U. Rehman, D. Hoekstra, I. S. Zuhorn, *ACS Nano* **2013**, *7*, 3767.
[28] A. Elouahabi, J. M. Ruysschaert, *Mol. Ther.* **2005**, *11*, 336.
[29] M. S. Al-Dosari, X. Gao, *AAPS J.* **2009**, *11*, 671.
[30] S. Fujita, R. Onuki-Nagasaki, J. Fukuda, J. Enomoto, S. Yamaguchi, M. Miyake, *Lab Chip* **2013**, *13*, 77.
[31] S. Kim, F. Qiu, S. Kim, A. Ghanbari, C. Moon, L. Zhang, B. J. Nelson, H. Choi, *Adv. Mater.* **2013**, *25*, 5863.
[32] F. Qiu, L. Zhang, S. Tottori, K. Marquardt, K. Krawczyk, A. Franco-Obregon, B. J. Nelson, *Mater. Today* **2012**, *15*, 463.
[33] B. Dalby, S. Cates, A. Harris, E. C. Ohki, M. L. Tilkins, P. J. Price, V. C. Ciccarone, *Methods* **2004**, *33*, 95.
[34] E. Delyagina, W. Li, N. Ma, G. Steinhoff, *Nanomedicine* **2011**, *6*, 1593.
[35] P. L. Felgner, T. R. Gadek, M. Holm, R. Roman, H. W. Chan, M. Wenz, J. P. Northrop, G. M. Ringold, M. Danielsen, *Proc. Natl. Acad. Sci. U.S.A.* **1987**, *84*, 7413.
[36] T. Yoshikawa, E. Uchimura, M. Kishi, D. P. Funeriu, M. Miyake, J. Miyake, *J. Controlled Release* **2004**, *96*, 227.
[37] J. Ziauddin, D. M. Sabatini, *Nature* **2001**, *411*, 107.
[38] E. Reimhult, F. Hook, B. Kasemo, *Langmuir* **2003**, *19*, 1681.
[39] K. E. Peyer, L. Zhang, B. J. Nelson, *Nanoscale* **2013**, *5*, 1259.
[40] L. Zhang, K. E. Peyer, B. J. Nelson, *Lab Chip* **2010**, *10*, 2203.